Appl. Phys. B 33, 187–193 (1984)

Applied Physics B Photophysics and Laser Chemistry

Self-Phase Locking in Lasers with Homogeneously Broadened Emission Lines

W. Brunner, R. Fischer, and H. Paul

Zentralinstitut für Optik und Spektroskopie, Akademie der Wissenschaften der DDR, Rudower Chaussee 6, DDR-1199 Berlin, German Democratic Republic

Received 12 August 1983/Accepted 5 October 1983

Abstract. It is shown by numerical analysis based on Lamb's equations of motion, that standing-wave lasers with purely homogeneously broadened emission lines exhibit regular multimode oscillations. Specifically, modes lying far from the line centre are quenched due to mode competition, and the amplitudes of the oscillating modes approach steady-state values. The stabilization of the amplitudes is normally accompanied, or followed, by an evolution of the phases towards a phase-locked regime, where the relative phases $\psi_n = 2\phi_n - \phi_{n+1} - \phi_{n-1}$ [ϕ_n phase in the n^{th} mode, defined by (6)] attain either the value 0 or $\pm\pi$. The build-up times for the relative phases are found to vary over a wide range.

PACS: 42.50, 42.55, 42.60

In preceding papers [1–3] we have studied theoretically, within the framework of Lamb's gas laser theory [4], mode competition effects in gas lasers in the presence of strong homogeneous line broadening, in addition to Doppler broadening. One interesting result was the prediction of a hysteresis effect in the transition between different stable two-mode regimes in Ar-ion lasers [1]. Furthermore, in case of multimode operation (more than two modes being oscillating) a chaotic behaviour has been found to exist for homogeneous linewidths that exceed the mode spacing [2, 3]: The amplitudes in the various modes undergo drastic changes in the course of time, and a stationary state with constant amplitudes, as predicted by the free-running approximation, is never reached.

In the present paper we extend our previous studies to the case of strong, purely homogeneous line broadening[1]. Such a situation will be realized, to a good approximation, in high-pressure CO_2 lasers, for instance. We again present numerical solutions of Lamb's equations of motion for lasers with Fabry-Perot type resonators that are completely filled with the active medium. It will be shown in the following that the behaviour of such a laser is quite different from the chaotic one described above: The amplitudes in the modes tend to stationary values and, in addition, their phases become normally locked, so that a steady-state is actually attained. This phase locking strongly affects the temporal behaviour of the total intensity.

[1] Risken and Nummedal [5] were the first to predict multimode operation in this case. In contrast to our present analysis, however, they considered a ring-resonator configuration and actually found the multimode regime to occur only very far above threshold

1. Basic Equations

Applying Lamb's formalism [4] to the case of a purely homogeneous laser line, we find the following equations of motion (cf. also [6])

$$\dot{\tilde{E}}_n = \tfrac{1}{2}\left(\frac{g_n}{\kappa} - 1\right)\tilde{E}_n - \sum_{\mu,\varrho,\sigma} \tilde{E}_\mu \tilde{E}_\varrho \tilde{E}_\sigma \delta_{\mu-\varrho+\sigma,n} \cdot [\cos\psi_{\mu\varrho\sigma n} G(\mu\varrho\sigma) - \sin\psi_{\mu\varrho\sigma n} F(\mu\varrho\sigma)], \tag{1}$$

$$\dot{\phi}_n \tilde{E}_n = \frac{g_n}{\kappa}\frac{\Omega-\omega_n}{2\gamma}\tilde{E}_n - \sum_{\mu,\varrho,\sigma} \tilde{E}_\mu \tilde{E}_\varrho \tilde{E}_\sigma \delta_{\mu-\varrho+\sigma,n} \cdot [\cos\psi_{\mu\varrho\sigma n} F(\mu\varrho\sigma) + \sin\psi_{\mu\varrho\sigma n} G(\mu\varrho\sigma)]. \tag{2}$$

Here, $\tilde{E}_n$ is the conveniently normalized amplitude in the n^{th} mode

$$\tilde{E}_n = \left(\frac{g\chi}{2\gamma^2\kappa}\right)^{1/2} E_n, \tag{3}$$

where E_n is the slowly varying amplitude of the electric field strength [Ref. 4, Eq. (11)], g is the gain at the line centre [see (5) below] and

$$\chi = \frac{p^2}{16\hbar^2} \tag{4}$$

denotes the coupling constant, p (assumed real) being the nondiagonal element for the electric dipole moment. The constant γ has the meaning of the homogeneous linewidth multiplied by π. [We allow for values of γ that are larger than $(\gamma_a+\gamma_b)/2$, where γ_a and γ_b are the reciprocal lifetimes of the upper and the lower atomic level, respectively, thus taking into account phase destroying processes like soft collisions.] The symbol g_n stands for the small-signal gain in the n^{th} mode

$$g_n = \frac{g}{1+\left(\dfrac{\Omega-\omega_n}{\gamma}\right)^2}, \tag{5}$$

where Ω is the circular frequency at the line centre and ω_n the (circular) frequency at which the n^{th} mode is oscillating. The quantity κ represents the cavity losses (assumed equal in all modes), and ϕ_n is defined by

$$\phi_n = (\omega_n - \Omega_n)t + \varphi_n(t), \tag{6}$$

where Ω_n is the cavity resonance frequency and $\varphi_n(t)$ the slowly varying phase for the n^{th} mode. Finally, the abbreviation

$$\psi_{\mu\varrho\sigma n} \equiv \phi_\mu - \phi_\varrho + \phi_\sigma - \phi_n \tag{7}$$

has been used.

The time is in units of κ^{-1}.

The coupling coefficients $F(\mu\varrho\sigma)$ and $G(\mu\varrho\sigma)$ are more complicated than in the Doppler limit [2, 3]. In explicit terms, they read

$$F(\mu\varrho\sigma) = \left\{ \frac{\gamma}{\gamma_a} \frac{\dfrac{\Omega-\omega_\mu+\omega_\varrho-\omega_\sigma}{\gamma}\dfrac{\omega_\sigma-\omega_\varrho}{\gamma_a}\dfrac{\Omega-\omega_\sigma}{\gamma} + \dfrac{\Omega-\omega_\mu+\omega_\varrho-\omega_\sigma}{\gamma} + \dfrac{\omega_\varrho-\omega_\sigma}{\gamma_a} + \dfrac{\Omega-\omega_\sigma}{\gamma}}{\left[1+\left(\dfrac{\Omega-\omega_\mu+\omega_\varrho-\omega_\sigma}{\gamma}\right)^2\right]\left[1+\left(\dfrac{\omega_\varrho-\omega_\sigma}{\gamma_a}\right)^2\right]\left[1+\left(\dfrac{\Omega-\omega_\sigma}{\gamma}\right)^2\right]} \right.$$

$$+ \frac{\gamma}{\gamma_a} \frac{\dfrac{\Omega-\omega_\mu+\omega_\varrho-\omega_\sigma}{\gamma}\dfrac{\omega_\varrho-\omega_\sigma}{\gamma_a}\dfrac{\Omega-\omega_\varrho}{\gamma} + \dfrac{\Omega-\omega_\mu+\omega_\varrho-\omega_\sigma}{\gamma} + \dfrac{\omega_\varrho-\omega_\sigma}{\gamma_a} + \dfrac{\omega_\varrho-\Omega}{\gamma}}{\left[1+\left(\dfrac{\Omega-\omega_\mu+\omega_\varrho-\omega_\sigma}{\gamma}\right)^2\right]\left[1+\left(\dfrac{\omega_\varrho-\omega_\sigma}{\gamma_a}\right)^2\right]\left[1+\left(\dfrac{\Omega-\omega_\varrho}{\gamma}\right)^2\right]}$$

$$\left. + \text{same with } \gamma_a \to \gamma_b \right\} (1+\delta_{\varrho\sigma}+\delta_{\mu\varrho}), \tag{8}$$

$$G(\mu\varrho\sigma) = \left\{ \frac{\gamma}{\gamma_a} \frac{1+\dfrac{\Omega-\omega_\mu+\omega_\varrho-\omega_\sigma}{\gamma}\dfrac{\omega_\sigma-\omega_\varrho}{\gamma_a} + \dfrac{\Omega-\omega_\mu+\omega_\varrho-\omega_\sigma}{\gamma}\dfrac{\omega_\sigma-\Omega}{\gamma} + \dfrac{\omega_\sigma-\omega_\varrho}{\gamma_a}\dfrac{\Omega-\omega_\sigma}{\gamma}}{\left[1+\left(\dfrac{\Omega-\omega_\mu+\omega_\varrho-\omega_\sigma}{\gamma}\right)^2\right]\left[1+\left(\dfrac{\omega_\varrho-\omega_\sigma}{\gamma_a}\right)^2\right]\left[1+\left(\dfrac{\Omega-\omega_\sigma}{\gamma}\right)^2\right]} \right.$$

$$+ \frac{\gamma}{\gamma_a} \frac{1+\dfrac{\Omega-\omega_\mu+\omega_\varrho-\omega_\sigma}{\gamma}\dfrac{\omega_\sigma-\omega_\varrho}{\gamma_a} + \dfrac{\Omega-\omega_\mu+\omega_\varrho-\omega_\sigma}{\gamma}\dfrac{\Omega-\omega_\varrho}{\gamma} + \dfrac{\omega_\varrho-\omega_\sigma}{\gamma_a}\dfrac{\Omega-\omega_\varrho}{\gamma}}{\left[1+\left(\dfrac{\Omega-\omega_\mu+\omega_\varrho-\omega_\sigma}{\gamma}\right)^2\right]\left[1+\left(\dfrac{\omega_\varrho-\omega_\sigma}{\gamma_a}\right)^2\right]\left[1+\left(\dfrac{\Omega-\omega_\varrho}{\gamma}\right)^2\right]}$$

$$\left. + \text{same with } \gamma_a \to \gamma_b \right\} (1+\delta_{\varrho\sigma}+\delta_{\mu\varrho}). \tag{9}$$

In the so-called free-running approximation [6], only those terms are retained in (1) for which $\psi_{\mu\varrho\sigma n}$ vanishes identically. Then (1) reduces to

$$\dot{\tilde{E}}_n = \tfrac{1}{2}\left(\frac{g_n}{\kappa} - 1\right)\tilde{E}_n - \tilde{E}_n \sum_i \tilde{E}_i^2 \theta_{ni}, \tag{10}$$

where

$$\theta_{nn} = G(nnn) = 6\gamma \frac{\gamma_a + \gamma_b}{\gamma_a \gamma_b} \frac{1}{\left[1 + \left(\frac{\Omega - \omega_n}{\gamma}\right)^2\right]^2}, \tag{11}$$

$$\begin{aligned}\theta_{ni} = \theta_{in} = G(nii) + G(iin) = {} & 4\gamma \frac{\gamma_a + \gamma_b}{\gamma_a \gamma_b} \frac{1}{\left[1 + \left(\frac{\Omega - \omega_n}{\gamma}\right)^2\right]\left[1 + \left(\frac{\Omega - \omega_i}{\gamma}\right)^2\right]} \\ & + 2\left\{ \frac{\gamma}{\gamma_a} \frac{1 + 2\frac{\omega_n - \Omega}{\gamma}\frac{\omega_i - \omega_n}{\gamma_a} - \left(\frac{\omega_n - \Omega}{\gamma}\right)^2}{\left[1 + \left(\frac{\Omega - \omega_n}{\gamma}\right)^2\right]^2 \left[1 + \left(\frac{\omega_i - \omega_n}{\gamma_a}\right)^2\right]} \right. \\ & + \frac{\gamma}{\gamma_a} \frac{1 + \frac{\omega_n - \Omega}{\gamma}\frac{\omega_i - \omega_n}{\gamma_a} + \frac{\omega_n - \Omega}{\gamma}\frac{\omega_i - \Omega}{\gamma} + \frac{\omega_i - \Omega}{\gamma}\frac{\omega_n - \omega_i}{\gamma_a}}{\left[1 + \left(\frac{\Omega - \omega_n}{\gamma}\right)^2\right]\left[1 + \left(\frac{\omega_i - \omega_n}{\gamma_a}\right)^2\right]\left[1 + \left(\frac{\Omega - \omega_i}{\gamma}\right)^2\right]} \\ & \left. + \text{same with } \gamma_a \to \gamma_b \right\}. \end{aligned} \tag{12}$$

Since the amplitude equations are decoupled from the phase equations, the latter need no longer be considered.

2. Details of the Numerical Treatment

The full system (1, 2) has been integrated numerically. In the calculations, the oscillation frequencies in (2, 5, 8, and 9) were replaced by the cavity resonance frequencies, which appears to be justified in the case of small cavity losses. For simplicity, we supposed the homogeneous linewidth to be mainly due to the decay of both the upper and the lower level, thus putting $\gamma = \frac{1}{2}(\gamma_a + \gamma_b)$. As in our previous work [2, 3], 13 modes labeled $n = 0, \pm 1, \ldots, \pm 6$ were taken into account in our computer program. In general, we assumed the mode $n = 0$ does not coincide with the line centre, but rather is displaced from it by a certain fraction of the mode spacing c, towards higher frequencies.

We examined numerically the evolution of the field amplitudes and phases in all the modes under consideration, starting from small amplitudes ($\tilde{E}_n = 10^{-4}$ for all modes) and random phases. In the calculations, the ratio of g and κ was held fixed, $g/\kappa = 1.2$. On the other hand, both the homogeneous linewidth in relation to the mode spacing $\Delta\omega$ ($= \Omega_{n+1} - \Omega_n$), and the ratio of the decay constants γ_a and γ_b were varied. The same holds for the parameter c. It turned out, however, that the results are rather insensitive to changes in c. Moreover, the evolution of the field (apart from its initial stage, of course) proved to be independent of the initial amplitudes.

3. Amplitude Stabilization

Rather surprisingly, the amplitudes do not exhibit any irregular behaviour (as it is the case in the presence of strong Doppler broadening, in addition to large homogeneous line broadening [2, 3]), instead they tend to stationary values in comparatively short times. As a consequence of mode competition a smaller number of modes are oscillating than would do so in the absence of mode coupling. Generally, such modes are quenched that are far from the line centre. Specifically, we found 3-mode oscillation to exist in certain circumstances (see Figs. 1a and 2a). Increasing the homogeneous linewidth leads to a larger number of oscillating modes (see Figs. 3a and 4a). This is easily understood as a

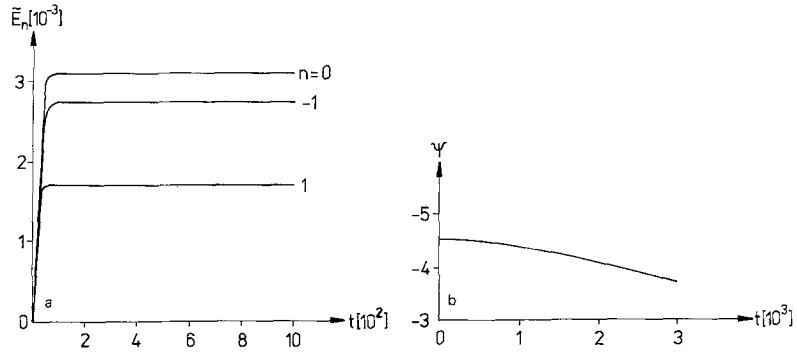

Fig. 1a and b. Evolution of the amplitudes (a) and the relative phase $\psi = 2\phi_0 - \phi_1 - \phi_{-1}$ (b) for $\Delta\omega/\gamma = 0.134$, $\Delta\omega/\gamma_a = 134.067$, $\Delta\omega/\gamma_b = 0.067$ ($\gamma_a/\gamma_b = 5 \times 10^{-4}$), $c = 0.25$. The number of modes N that would oscillate in the absence of coupling is 7. (The time is in units of κ^{-1})

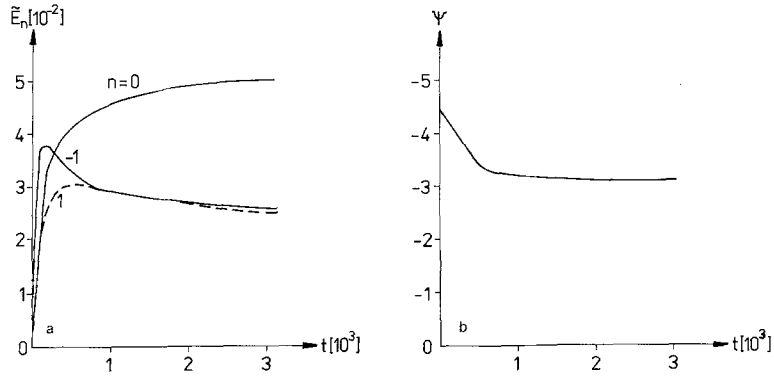

Fig. 2a and b. Same as Fig. 1 for $\Delta\omega/\gamma = 0.067$, $\Delta\omega/\gamma_a = 0.25$, $\Delta\omega/\gamma_b = 0.039$ ($\gamma_a/\gamma_b = 0.16$), $c = 0.25$; $N = 13$

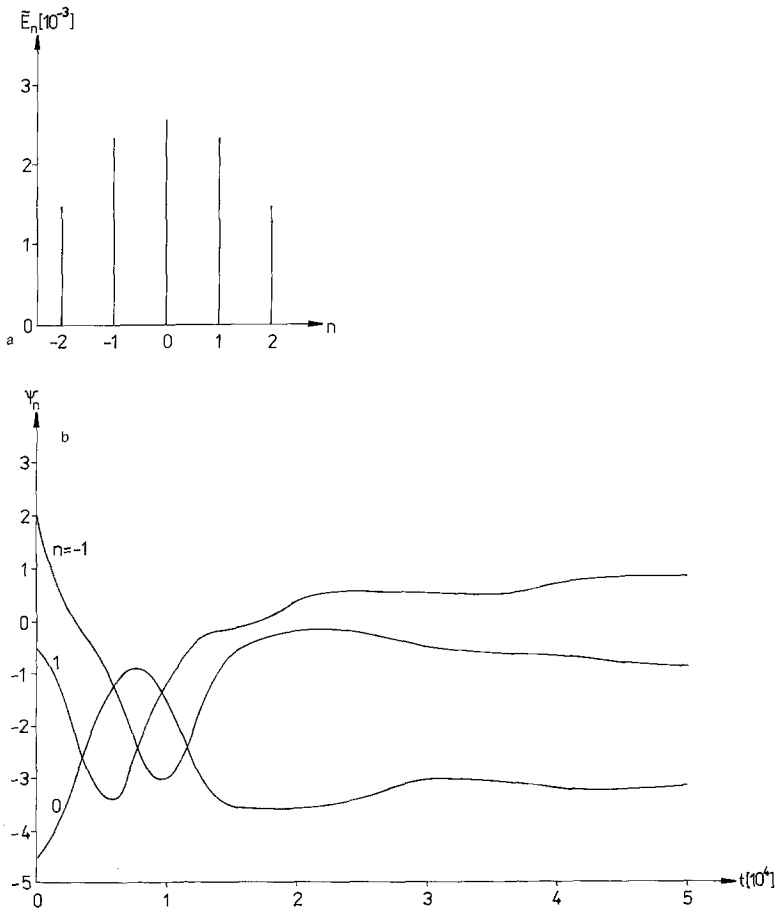

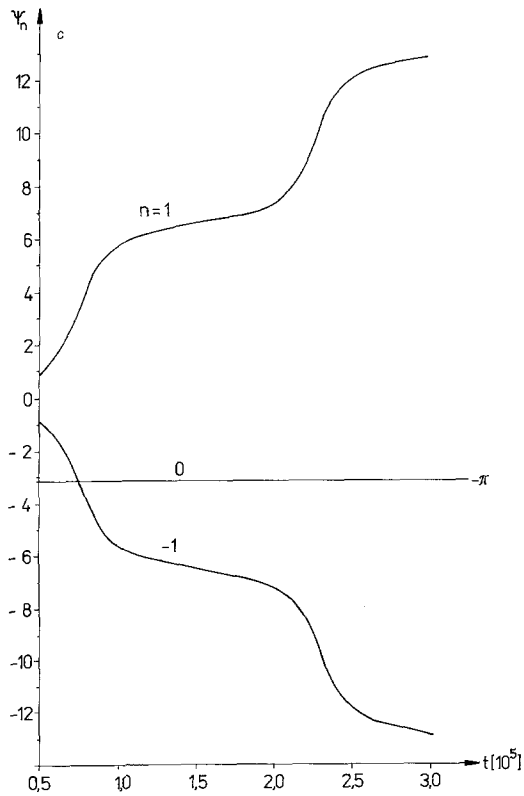

Fig. 3a–c. Steady-state amplitudes (a) and evolution of the relative phases $\psi_n = 2\phi_n - \phi_{n+1} - \phi_{n-1}$ (b) and (c) for $\Delta\omega/\gamma = 0.067$, $\Delta\omega/\gamma_a = 67.034$, $\Delta\omega/\gamma_b = 0.0335$ ($\gamma_a/\gamma_b = 5 \times 10^{-4}$), $c = 0$; $N = 13$

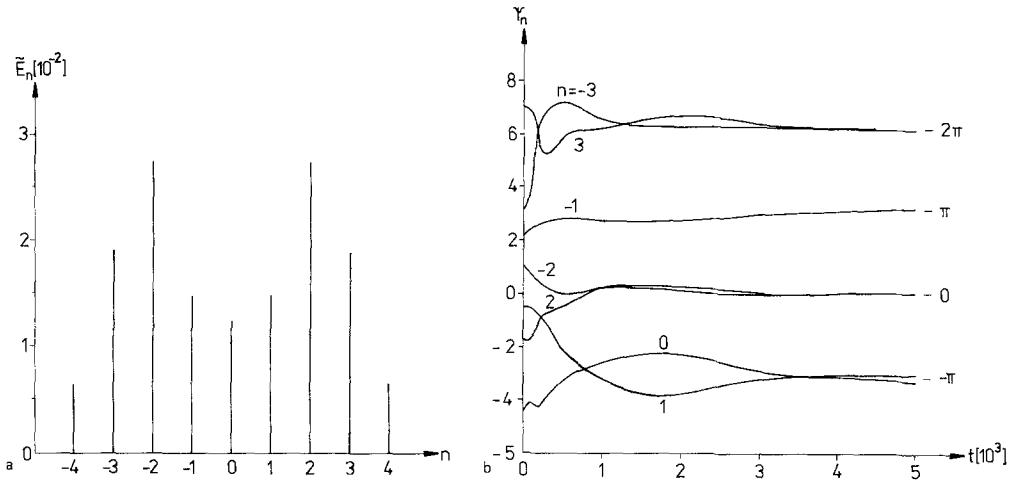

Fig. 4a and b. Same as Fig. 3 for $\Delta\omega/\gamma = 0.035$, $\Delta\omega/\gamma_a = 0.1925$, $\Delta\omega/\gamma_b = 0.01925$ $(\gamma_a/\gamma_b = 0.1)$, $c = 0$; $N = 25$

consequence of the corresponding broadening of the gain profile (5), as a function of n. At the same time, there is a tendency for the number of oscillating modes to get increased, when γ_a and γ_b differ more and more. This is seen by comparing Figs. 2a and 3a.

It should be noted that within any group of oscillating modes there are no "holes" (corresponding to suppressed modes). This is in a marked contrast to the situation encountered in the Ar-ion laser case [1]. When only a few modes oscillate, the mode nearest to the line centre has the greatest amplitude. This is, however, not the case for a larger number of oscillating modes ($\gtrsim 9$), as becomes evident from Fig. 4a.

For comparison, we performed also calculations in the free-running approximation (10). In this case, single-mode operation was predicted quite generally (the mode nearest to the line centre quenched all the remaining ones). Hence, the free-running approximation cannot be applied, and it becomes obvious that the phase terms in the basic equations (1 and 2) play an important role.

4. Phase Locking

Our numerical analysis revealed that normally the amplitude stabilization is accompanied, or followed, by an evolution of the phases towards a phase-locked regime. Hence a steady-state is attained. Its existence is, in fact, compatible with the equations of motion [Ref. 6, p. 134], however, it is by no means trivial that the latter allow for *stable* stationary solutions.

4.1. Three-Mode Operation

In the 3-mode case, a detailed analytical treatment of the locking phenomenon has been given in [Ref. 6, p. 129], which is based, however, on the assumption that the variations in the amplitudes can be neglected ("decoupled approximation").

In the following, we first briefly reproduce, in our notation, the theoretical results derived in [6]. It follows from (2), by simple algebra, that

$$\frac{d\psi}{dt} = d + l_s \sin\psi + l_c \cos\psi \equiv d + l \sin(\psi - \psi_0), \tag{13}$$

where

$$\psi = 2\phi_0 - \phi_1 - \phi_{-1}, \tag{14}$$

$$d = \frac{1}{2\kappa\gamma}[2g_0(\Omega-\omega_0) - g_1(\Omega-\omega_1) - g_{-1}(\Omega-\omega_{-1})] + \sum_{i=-1}^{+1} \tilde{E}_i^2 \{F(ii-1) + F(-1ii) + F(ii1) + F(1ii) - 2[F(ii0) + F(0ii)]\} + 2\tilde{E}_0^2 F(000) - \tilde{E}_1^2 F(111) - \tilde{E}_{-1}^2 F(-1-1-1), \tag{15}$$

$$l_s = 2\tilde{E}_{-1}\tilde{E}_1[G(-101) + G(10-1)] + \tilde{E}_0^2\left[\frac{\tilde{E}_{-1}}{\tilde{E}_1} G(0-10) + \frac{\tilde{E}_1}{\tilde{E}_{-1}} G(010)\right], \tag{16}$$

$$l_c = -2\tilde{E}_{-1}\tilde{E}_1[F(-101) + F(10-1)] + \tilde{E}_0^2\left[\frac{\tilde{E}_{-1}}{\tilde{E}_1} F(0-10) + \frac{\tilde{E}_1}{\tilde{E}_{-1}} F(010)\right], \tag{17}$$

$$\psi_0 = -\arctan\frac{l_c}{l_s}, \tag{18}$$

$$l = l_s\sqrt{1 + \left(\frac{l_c}{l_s}\right)^2}. \tag{19}$$

For convenience, we have labeled the modes $-1, 0, 1$; of course, the above results hold for any three neighbouring modes. While the analysis in [6] was restricted to the discussion of the stationary case ($d\psi/dt = 0$), we investigate more generally the approach to the steady

state. In fact, (13) can be integrated, for $|d/l|<1$, to yield (cf. also [7])

$$\psi-\psi_0=2\arctan\left\{-\frac{l}{d}+\frac{l}{d}\sqrt{1-\left(\frac{d}{l}\right)^2}\,\frac{1+a\exp\left[\sqrt{1-\left(\frac{d}{l}\right)^2}\,lt\right]}{1-a\exp\left[\sqrt{1-\left(\frac{d}{l}\right)^2}\,lt\right]}\right\}, \tag{20}$$

where the abbreviation

$$a=\frac{\frac{d}{l}\tan\left(\frac{\psi(0)-\psi_0}{2}\right)+1-\sqrt{1-\left(\frac{d}{l}\right)^2}}{\frac{d}{l}\tan\left(\frac{\psi(0)-\psi_0}{2}\right)+1+\sqrt{1-\left(\frac{d}{l}\right)^2}} \tag{21}$$

has been introduced.

In the cases studied in our numerical analysis, the inequalities $|d|\ll|l|$ and $|l_c|\ll|l_s|$ were fulfilled. In these circumstances (20) becomes very simple; to a good approximation, it reduces to

$$\psi(t)=2\arctan\left\{\tan\left(\frac{\psi(0)}{2}\right)e^{lt}\right\}. \tag{22}$$

It is evident from (22) that the steady-state value of ψ is determined by the sign of l:

$$\psi(\infty)=\begin{cases}0 & \text{for } l<0\\ \pm\pi & \text{for } l>0.\end{cases} \tag{23}$$

In the first case one speaks of amplitude modulation (AM) phase locking, the second one has been termed frequency modulation (FM) mode locking [Ref. 6, p. 132].

The result (23) is the same as that obtained in [6; Eq. (22)], however, provides additional information about the time needed to actually attain the steady-state.

Our numerical results presented in Figs. 1b–4b are, in fact, in quantitative agreement with the prediction (22). In Fig. 1b the parameters were chosen such that $l<0$. Hence ψ tends to zero, however, $|l|$ is so small that the evolution proceeds rather slowly, and one recognizes that the "decoupled approximation" works excellently in these circumstances. In Fig. 2b, ψ approaches much faster its stationary value which equals $-\pi$, since l is now positive.

4.2. *Multimode Operation*

Interestingly, we found also in case of multimode operation that the relative phases

$$\psi_n=2\phi_n-\phi_{n+1}-\phi_{n-1} \tag{24}$$

(but not necessarily all of them) attained stationary values which proved to be either 0 or $\pm\pi$, as in the 3-mode case.

This is illustrated by Figs. 3b and c and 4b.

It should be noted that the relative phases ψ evolve on different time scales. One recognizes from Figs. 3b and c and 4b that the monotonic approach to the steady-state, as expressed by formula (22), is not a general rule. Moreover, Fig. 3b and c reveal that only partial mode locking may take place. This does not affect, however, the steady-state amplitudes which, in fact, are practically attained when a time t of a few hundreds (in units of κ^{-1}) has elapsed.

5. Time Behaviour of the Total Intensity

It is well known that the total intensity depends critically on the phases of the different oscillating modes. For illustration of this point, the total intensity has been plotted for the multimode oscillation represented by Fig. 4. Figure 5a shows its temporal behaviour in the steady-state. It is interesting to see that it varies only slightly. On the other hand, replacement of the actual (steady-state) phases by $\phi_n=0$ (perfect AM phase locking) yields excellent pulses (see Fig. 5b). To demonstrate how strongly the evolution of the phases affects the total intensity, we have associated the steady-state amplitudes with the (random) initial phases too. The result is shown in Fig. 5c.

In conclusion, we have shown by numerical analysis that in case of strong, purely homogeneous line broadening the oscillating modes exhibit a regular behaviour; The amplitudes tend to stationary values, while the phases normally become locked. Hence, a steady-state is attained.

Thus it is proved that *stable* stationary solutions to the equations of motion actually exist.

This is in contrast to the situation encountered in the case of strong homogeneous line broadening, in the presence, however, of dominating Doppler broadening, where (except stable two-mode oscillation [1]) the

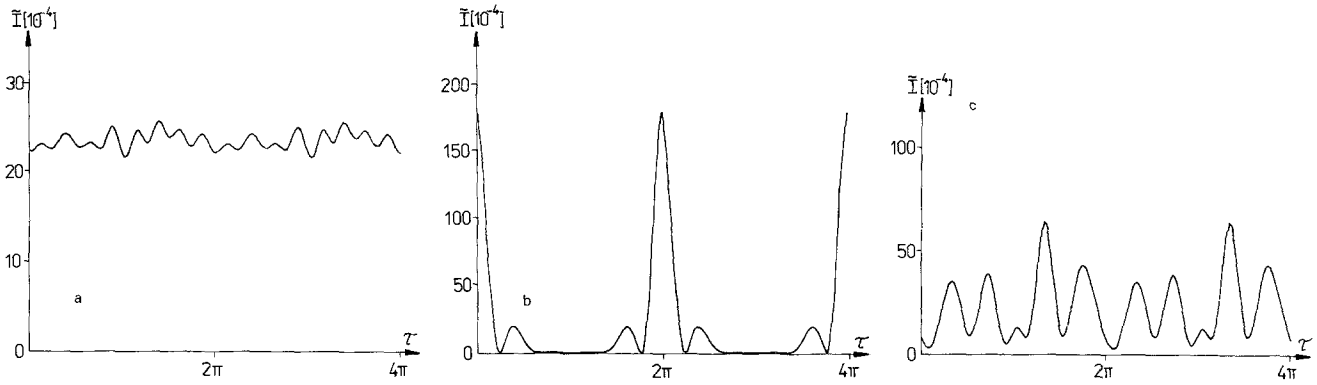

Fig. 5a–c. Total normalized intensity $\tilde{I}(\tau) = \sum_{n,m} E_n E_m \cos[(n-m)\tau + \phi_n - \phi_m]$ vs. time τ (in units of the reciprocal mode spacing $\Delta\omega^{-1}$) corresponding to the steady-state amplitudes taken from Fig. 4a and a set of locked phases in accordance with the steady-state values for ψ_n in Fig. 4b (a), the phases $\phi_n = 0$ (b), and the initial (random) phases (c)

multimode oscillations are of chaotic character [2, 3]. From this result it appears rather surprising that the stronger mode coupling connected with purely homogeneous line broadening produces order rather than chaos.

Acknowledgements. We are grateful to Dipl.-Math. T. Reiher for preparing the computer program, and to Dr. J. Tilgner for assistance in the numerical work.

References

1. W. Brunner, H. Paul: Opt. Commun. **35**, 421 (1980)
2. W. Brunner, H. Paul: Opt. Quantum Electron. **15**, 87 (1983)
3. W. Brunner, R. Fischer, H. Paul, Dinh van Hoang: Kvant. Elektron. (Moscow) **10**, 103 (1983)
4. W.E. Lamb, Jr.: Phys. Rev. **134**, A 1429 (1964)
5. H. Risken, K. Nummedal: J. Appl. Phys. **39**, 4662 (1968)
6. M. Sargent III, M.O. Scully, W.E. Lamb, Jr.: *Laser Physics* (Addison-Wesley, Reading, MA 1974)
7. H. Dekker: Appl. Phys. **4**, 257 (1974)

Responsible for Advertisements: E. Lückermann, G. Probst, Kurfürstendamm 237, D-1000 Berlin 15, Telephone: (0 30) 8 82 10 31, Telex 01-85411
Responsible for the Text: H. K. V. Lotsch, Tiergartenstrasse 17, D-6900 Heidelberg. Printers: Brühlsche Universitätsdruckerei, Giessen, Printed in Germany